# The Clairaut Equation and Its Connection to Satellite Geodesy and Planetology

P. Lanzano* and J. C. Daley†
*U.S. Naval Research Laboratory, Washington, D.C.*

**The Clairaut equation for rotating bodies in hydrostatic equilibrium was integrated numerically up to its third-order approximation using the 1969 Haddon-Bullen Earth's density model. The computations, based on finite-difference methods, were executed in double precision on the Texas Instruments ASC-7 computer. The results are: 1) the coefficients of the second, fourth, and sixth harmonic of the geopotential, and 2) the geoid to the same approximation inclusive of its moments of inertia and ellipticity. It is suggested that the newly determined geoid be used as the reference surface in gravimetric work. The results are compared with Kopal's 1963 work based on the 1940 Bullen density model and second-order approximation. Discrepancies with satellite geodesy are attributed to shear stresses in the Earth's interior because of convection currents. To better compare our density-based results with satellite geodesy, we analytically obtained expressions for the secular variations of the elements of a Keplerian orbit, and advocate that the formulas be used to evaluate the harmonics from satellite data. The Clairaut equation also can be applied to Jupiter by assuming the planet to be a rotating polytrope and solving a nonhomogeneous Lane-Emden equation to determine its density.**

## I. Introduction

THE purpose of this paper is to describe the numerical integration of the Clairaut equation up to its third-order approximation for a rotating, axially symmetric Earth when its density distribution is assumed to be the 1969 $HB_1$ model of Haddon and Bullen. We shall discuss briefly applications of this equation to satellite geodesy and planetology. To afford a complete comparison with results obtainable from satellite data, we have ascertained in a rigorous manner the secular variations of the orbital elements of a Keplerian elliptic orbit due to the coefficients of the second, fourth, and sixth harmonic in the geopotential.

Consider a deformable, massive body of arbitrary density, rotating uniformly about an axis. Assume hydrostatic equilibrium; assume also that, because of the rotation, the original spherical shape of the body will be deformed into a spheroid possessing axial symmetry and symmetry with respect to the equatorial plane. Let $r$ denote the radial distance from the centroid 0 of the body and $a$ denote the mean radius of an equipotential spheroid. This family of surfaces can be represented by the equation

$$\frac{r(a,\nu)}{a} = 1 + \sum_{j=0}^{3} f_{2j}(a) P_{2j}(\nu) + \ldots \tag{1}$$

where the $P$'s are the Legendre polynomials and $\nu = \cos\theta$ is the cosine of the polar distance. Let $\omega_l$ represent the angular velocity of rotation, $m_l$ the total mass of the body, $a_l$ the mean radius of the outermost spheroid, and $G$ the gravitational constant. We define then the dimensionless rotational parameter

$$q = \omega_l^2 a_l^3 / 3Gm_l \tag{2}$$

which is essentially the ratio between the centrifugal and gravitational accelerations of the body. For the Earth, $q = 0.00115$. In terms of this parameter, the deformation coefficients $f_j(a)$ can be expressed as

$$f_0 = q^2 f_{02} + q^3 f_{03} \tag{3a}$$

$$f_2 = q f_{21} + q^2 f_{22} + q^3 f_{23} \tag{3b}$$

$$f_4 = q^2 f_{42} + q^3 f_{43} \tag{3c}$$

$$f_6 = q^3 f_{63} \tag{3d}$$

In a recent paper,[1] we have established a third-order theory which ascertains the differential equations satisfied by the functions $f_{jk}(a)$. We summarize here the essential results which are required for numerical integration purposes, with the reminder that full details are available in the aforementioned reference. $f_{02}$ and $f_{03}$ are eliminated through mass conservation considerations; it turns out that

$$f_0 = -1/5 q^2 f_{21}^2 - 2/5 q^3 f_{21} (f_{22} + 1/21 f_{21}^2) \tag{4}$$

The other six deformation coefficients, i.e., $f_{21}$, $f_{22}$, $f_{23}$, $f_{42}$, $f_{43}$, and $f_{63}$ are solutions of the Clairaut equations in its various approximations

$$a^2 f'' + 6aDf' + (6D - C)f = R \tag{5}$$

satisfying also boundary conditions

$$f(0) = f'(0) = 0 \tag{6a}$$

$$Af(a_l) + Bf'(a_l) = S(a_l) \tag{6b}$$

at both ends of the integration interval. The primes denote derivatives with respect to the mean radius $a$, and $A$, $B$, and $C$ are constants depending on the approximation. The function

$$D(a) = \rho(a)/\bar{\rho}(a) \tag{7}$$

is the ratio between the density $\rho(a)$ and the mean density

$$\bar{\rho}(a) = \frac{3}{a^3} \int_0^a \rho a^2 da \tag{8}$$

Received Dec. 28, 1976; presented as Paper 77-69 at the AIAA 15th Aerospace Sciences Meeting, Los Angeles, Calif., Jan. 24-26, 1977; revision received May 31, 1977.

Index categories: Atmospheric and Space Sciences; Earth-Orbital Trajectories; Analytical and Numerical Methods.

*Senior Research Scientist, Space Systems Division. Associate Fellow AIAA.

†Head, Digital Applications Section, Space Systems Division. Member AIAA.

$R(a)$ and $S(a)$ are known functions of $a$ depending on lower-order approximations; in particular $R_{2l}=0$. By introducing the logarithmic derivative

$$\eta = af'/f \tag{9}$$

and noting that

$$a^2 f''/f = a\eta' - \eta(1-\eta)$$

one can transform the Clairaut equation into the Radau equation

$$a\eta' + 6D\eta - \eta(1-\eta) = T \tag{10}$$

Equations (5) and (10) are completely equivalent, their numerical integration can be achieved only if the density distribution $\rho(a)$ is known. The Earth's density distribution is obtainable from seismological evidence. In what follows, we provide a few details about the Haddon-Bullen density model and the earlier Bullen model.

## II. $HB_1$ Earth Density Model

Let $\rho$, $k$, $\mu$, $\alpha$, and $\beta$ denote the density, incompressibility, rigidity, and the $P$ and $S$ seismic velocities at depth $z$ below the surface of an Earth model, or at a distance $r$ from the center. It is known then[2] that

$$\alpha^2 = \frac{k}{\rho} + \frac{4}{3}\beta^2; \quad \beta^2 = \frac{\mu}{\rho}; \quad \frac{d\rho}{dz} = \eta\rho^2\frac{g}{k} \tag{11}$$

where $g$ is the acceleration of gravity and $\eta$ is a coefficient depending on the homogeneity of the material. An Earth model is supposed to be known when either set $(\rho,\alpha,\beta)$ or $(\rho,k,\mu)$ is specified for every $z$. A spherical symmetric model can represent only an average Earth structure. As early as 1940 Bullen obtained an Earth model from seismic bodily wave data alone by connecting the travel time $t$ with the angular distance $\Delta$ and using Eqs. (11). James and Kopal[3] used this early Bullen density model to ascertain the geometric figure of the Earth.

The 1969 $HB_1$ model[4] is the latest developed model and takes into account the following facts: 1) free Earth oscillation data consisting of 110 observations of periods of fundamental spheroidal and torsional oscillations corresponding to order numbers $n$ with $0 \le n \le 48$ and $2 \le n \le 44$, respectively, and of the first and second spheroidal overtones for $n \le 20$ (these data include the results of the Chilean and Alaskan earthquakes of May 1960 and March 1964); 2) the revised value of the Earth's polar moment of interia $I_p$ according to the relation

$$I_p = 0.3309\, m_l a_l^2 \tag{12}$$

where $m_l = 5.976 \cdot 10^{27}$ $g$ is the Earth's total mass and $a_l = 6371$ km is the Earth's mean radius (i.e., the radius of a sphere of equal volume); 3) the newly established evidence that the central density $\rho_c$ is $\le 13$ g/cm$^3$. The $HB_1$ model was obtained as a parametric modification of the earlier version by varying the parameters singly or in groups, within plausible limits and testing the resulting model against the oscillation observations and the other physical evidence. Although not expected to be the final Earth model, it is, however, acknowledged that certain of its features seem to be fairly well established. The main features of $HB_1$ with respect to the earlier model are: 1) reduced crustal thickness from 33 to 15 km; 2) more complex layering of the upper mantle; 3) increased core radius by 20 km to 3493 km; and 4) no important changes in the $\alpha$ profile from the Jeffreys data.

Table 1 furnishes the values of $\rho$ in g/cm$^3$, $\alpha$ and $\beta$ in km/sec for appropriate values of the depth $z$ in km, as well as the density related function $D$. The model has nine layers,

**Table 1 Values of density $\rho$, $D=\rho/\bar{\rho}$, $P$ velocity $\alpha$, and $S$ velocity $\beta$ in Earth model $HB_1$**

| Depth (km) | $\rho$ (g/cm$^3$) | D | $\alpha$ (km/sec) | $\beta$ (km/sec) |
|---|---|---|---|---|
| 0 | 2.840 | 0.5147 | 6.300 | 3.550 |
| 15 | 2.840 | 0.5129 | 6.300 | 3.550 |
| 15 | 3.313 | 0.5983 | 7.696 | 4.625 |
| 60 | 3.332 | 0.5966 | 7.831 | 4.625 |
| 60 | 3.332 | 0.5966 | 7.831 | 4.500 |
| 100 | 3.348 | 0.5949 | 7.951 | 4.500 |
| 200 | 3.387 | 0.5901 | 8.256 | 4.500 |
| 300 | 3.424 | 0.5846 | 8.585 | 4.500 |
| 350 | 3.441 | 0.5815 | 8.750 | 4.500 |
| 350 | 3.700 | 0.6252 | 8.750 | 4.500 |
| 400 | 3.775 | 0.6320 | 8.924 | 4.717 |
| 413 | 3.795 | 0.6337 | 8.970 | 4.774 |
| 500 | 3.925 | 0.6452 | 9.650 | 5.150 |
| 600 | 4.075 | 0.6579 | 10.243 | 5.583 |
| 650 | 4.150 | 0.6642 | 10.481 | 5.800 |
| 650 | 4.200 | 0.6722 | 10.481 | 5.900 |
| 800 | 4.380 | 0.6832 | 11.009 | 6.149 |
| 984 | 4.529 | 0.6844 | 11.420 | 6.351 |
| 1000 | 4.538 | 0.6839 | 11.440 | 6.362 |
| 1200 | 4.655 | 0.6764 | 11.706 | 6.500 |
| 1400 | 4.768 | 0.6664 | 11.992 | 6.622 |
| 1600 | 4.877 | 0.6537 | 12.262 | 6.730 |
| 1800 | 4.983 | 0.6382 | 12.530 | 6.829 |
| 2000 | 5.087 | 0.6199 | 12.794 | 6.924 |
| 2200 | 5.188 | 0.5985 | 13.034 | 7.018 |
| 2400 | 5.288 | 0.5739 | 13.270 | 7.117 |
| 2600 | 5.387 | 0.5461 | 13.495 | 7.214 |
| 2800 | 5.487 | 0.5152 | 13.638 | 7.312 |
| 2878 | 5.527 | 0.5023 | 13.642 | 7.310 |
| 2878 | 9.927 | 0.9022 | 8.106 | 0.000 |
| 3000 | 10.121 | 0.9107 | 8.247 | 0.000 |
| 3200 | 10.421 | 0.9236 | 8.496 | 0.000 |
| 3400 | 10.697 | 0.9351 | 8.791 | 0.000 |
| 3600 | 10.948 | 0.9452 | 9.059 | 0.000 |
| 3800 | 11.176 | 0.9541 | 9.307 | 0.000 |
| 4000 | 11.383 | 0.9619 | 9.531 | 0.000 |
| 4200 | 11.570 | 0.9688 | 9.731 | 0.000 |
| 4400 | 11.737 | 0.9748 | 9.907 | 0.000 |
| 4600 | 11.887 | 0.9802 | 10.096 | 0.000 |
| 4800 | 12.017 | 0.9847 | 10.284 | 0.000 |
| 4982 | 12.121 | 0.9884 | 10.468 | 0.000 |
| 5000 | 12.130 | 0.9887 | 10.332 | 0.000 |
| 5121 | 12.197 | 0.9914 | 9.428 | 0.000 |
| 5121 | 12.197 | 0.9914 | 11.188 | 0.000 |
| 5200 | 12.229 | 0.9925 | 11.205 | 0.000 |
| 5400 | 12.301 | 0.9948 | 11.243 | 0.000 |
| 5600 | 12.360 | 0.9968 | 11.275 | 0.000 |
| 5800 | 12.405 | 0.9982 | 11.300 | 0.000 |
| 6000 | 12.437 | 0.9993 | 11.320 | 0.000 |
| 6200 | 12.455 | 0.9998 | 11.332 | 0.000 |
| 6371 | 12.460 | 1.0000 | 11.338 | 0.000 |

separated by boundaries at the depths 15, 60, 350, 650, 984, 2878, 4982, and 5121 km, which are referred to as crustal layer $A$, mantle layers $B'$, $B''$, $C'$, $C''$, and $D$, and the core layers $E$, $F$, and $G$. A short description of the model is as follows: 1) the values of $\rho$, $\alpha$, $\beta$ remain constant throughout the crust, 2) $\alpha$ has discontinuities at $z=15$, 2878, and 5121 km; $d\alpha/dz$ has discontinuities at $z=413$ and 4982 km; 3) $\beta$ has the constant value 4.625 km/sec in the $B'$ layer, and the value 4.5 km/sec in the $B''$ layer; $\beta$ varies linearly in $C'$ and quadratically in $C''$; both $\beta$ and $d\beta/dz$ are continuous at $z=984$ km; the Jeffreys values for $\beta$ have been preserved in the $D$ layer; and, finally, $\beta=0$ in the core; 4) the density $\rho$ takes the constant value 2.84 g/cm$^3$ throughout the entire crust; its value jumps by 0.47 g/cm$^3$ at $z=15$ km; $\rho$ remains continuous and varies nearly linearly according to Eq. (11) with $\eta=0.45$ in the $B'+B''$ layers; the density jumps by 0.26 g/cm$^3$ at the $B''$ $C'$ boundary; $\rho$ varies linearly in $C'$; density jumps by 0.05 g/cm$^3$ at the $C'$ $C''$ boundary; $\rho$ varies quadratically in $C''$, $\rho$ and $d\rho/dz$ are continuous at $z=984$ km; $d\rho/dz$ is determined from Eq. (11) with $\eta=1$ throughout the $D$ layer and the whole core; at $z=2878$ km the value of $\rho$ jumps by 4.4 g/cm$^3$; finally, $\rho_c=12.46$ g/cm$^3$.

## III. Numerical Integration of the Clairaut Equation with Discontinuous Coefficients

The numerical integration of the six Clairaut equations has been performed by means of finite-difference methods. Since the density model exhibits four discontinuities, so also the function $D(a)$ has discontinuities at those same points.

The computation of $D$ presents no problem. By piecewise integration, the mean density at any point $a$ over a range which includes a discontinuity at $c$ is calculated according to

$$\bar{\rho}(a) = \frac{3}{a^3}\left(\int_0^c \rho a^2 da + \int_c^a \rho a^2 da\right) \tag{13}$$

At the point of discontinuity $c$, one has

$$\bar{\rho}(c) = \frac{3}{a^3} \int_0^c \rho a^2 \mathrm{d}a \tag{14}$$

so that the value of $D$ at $c$, approaching from the left ($L$) and from the right ($R$), can be written as

$$D_L(c) = \rho_L(c)/\bar{\rho}(c)$$

$$D_R(c) = \rho_R(c)/\bar{\rho}(c)$$

This procedure can be extended easily to the case where more than one discontinuity is present, as is the case in the $HB_1$ model. The integrals in Eqs. (13) and (14) were calculated by the Romberg method using a subroutine adapted from McCalla.[5] Intermediate values of $\rho(a)$ were obtained using a second-degree Lagrange interpolation between the data points, and the integration was carried out to a tolerance of $5 \cdot 10^{-7}$. The function $D(a)$ then is obtained and saved at all points which will be required later; its accuracy is independent of the choice of interval in the finite-difference scheme.

Using central difference formulas for first and second derivatives within an interval of length $H$, the finite-difference form of the Clairaut equation at a pivotal point $a_i^*$ is

$$\left(1 - \frac{3H}{a_i^*} D_i\right) f_{i-1} + \left[-2 + \left(\frac{H}{a_i^*}\right)^2 \left(6D_i - C\right)\right] f_i + \left(1 + \frac{3H}{a_i^*} D_i\right) f_{i+1} = \left(\frac{H}{a_i^*}\right)^2 R_i \tag{15}$$

having neglected the third and higher order central difference terms.[6] We select the pivotal points $a_i^*$, $i = 1, \ldots, N$ at equal intervals to include the boundary points $a = 0$ and $a = a_1$. This choice requires the value of $f$ at two points external to the interval in consideration. These "external" points, however, can be eliminated by using both boundary conditions. Thus, the condition $f'(0) = 0$ at $a = a_1^* = 0$, in terms of finite differences, can be written as $f_0 = f_2$. Substituting it into the first equation with $D_1 = 1$, we obtain

$$(4 - C)f_1 + 2f_2 = R_1$$

for the first equation (pivotal point at $a = 0$). By a similar procedure, the external point at the surface side is eliminated. For $i = 2, \ldots, N-1$ and equal intervals, $a_i^* = (i-1)H$, and the system of Eqs. (15) can be written as

$$A(i,1)f_{i-1} + A(i,2)f_i + A(i,3)f_{i+1} = A(i,4) \tag{16}$$

where

$$A(i,1) = 1 - 3D_i/(i-1) \tag{17a}$$

$$A(i,2) = -2 + (6D_i - C)/(i-1)^2 \tag{17b}$$

$$A(i,3) = 1 + 3D_i/(i-1) \tag{17c}$$

$$A(i,4) = R_i/(i-1)^2 \tag{17d}$$

Prior to solving the linear system of Eq. (16), we must take into account the fact that the coefficients of the original differential equation have discontinuities. Two cases can occur: 1) the discontinuity coincides with a pivotal point, or 2) the discontinuity appears at an arbitrary location relative to the equally spaced pivotal points. We have followed a technique detailed in Fox[6] to insure a unique solution by imposing extra conditions. Thus, by assuming continuity for

**Table 2 Deformation coefficients for the equipotential surfaces and their logarithmic derivatives**

| $a$ (km) | $-10^6 \cdot f_0$ | $\eta_0$ | $-10^2 \cdot f_2$ | $\eta_2$ | $+10^5 \cdot f_4$ | $\eta_4$ | $-10^8 \cdot f_6$ | $\eta_6$ |
|---|---|---|---|---|---|---|---|---|
| 0 | .54147 | 0.0000 | .16455 | 0.0000 | .20887 | 0.0000 | .25878 | 0.0000 |
| 171 | .54155 | 0.0003 | .16457 | 0.0001 | .20891 | 0.0004 | .25889 | 0.0008 |
| 371 | .54182 | 0.0013 | .16461 | 0.0006 | .20907 | 0.0019 | .25927 | 0.0037 |
| 571 | .54229 | 0.0030 | .16468 | 0.0015 | .20934 | 0.0045 | .25994 | 0.0090 |
| 771 | .54297 | 0.0055 | .16478 | 0.0028 | .20973 | 0.0082 | .26090 | 0.0163 |
| 971 | .54385 | 0.0088 | .16492 | 0.0044 | .21023 | 0.0131 | .26215 | 0.0260 |
| 1171 | .54495 | 0.0129 | .16508 | 0.0065 | .21086 | 0.0191 | .26370 | 0.0378 |
| 1250 | .54544 | 0.0147 | .16516 | 0.0074 | .21114 | 0.0218 | .26440 | 0.0431 |
| 1371 | .54626 | 0.0181 | .16528 | 0.0091 | .21161 | 0.0268 | .26557 | 0.0533 |
| 1389 | .54639 | 0.0187 | .16530 | 0.0094 | .21169 | 0.0277 | .26576 | 0.0551 |
| 1571 | .54786 | 0.0251 | .16552 | 0.0126 | .21253 | 0.0370 | .26786 | 0.0731 |
| 1771 | .54977 | 0.0332 | .16581 | 0.0166 | .21361 | 0.0483 | .27055 | 0.0949 |
| 1971 | .55198 | 0.0423 | .16614 | 0.0212 | .21486 | 0.0612 | .27366 | 0.1195 |
| 2171 | .55451 | 0.0527 | .16652 | 0.0264 | .21628 | 0.0758 | .27720 | 0.1474 |
| 2371 | .55737 | 0.0645 | .16695 | 0.0322 | .21788 | 0.0921 | .28120 | 0.1786 |
| 2571 | .56058 | 0.0778 | .16743 | 0.0389 | .21968 | 0.1106 | .28569 | 0.2136 |
| 2771 | .56416 | 0.0928 | .16797 | 0.0464 | .22167 | 0.1313 | .29071 | 0.2528 |
| 2971 | .56815 | 0.1097 | .16856 | 0.0549 | .22388 | 0.1546 | .29631 | 0.2966 |
| 3171 | .57257 | 0.1289 | .16921 | 0.0645 | .22634 | 0.1808 | .30256 | 0.3458 |
| 3371 | .57747 | 0.1506 | .16994 | 0.0753 | .22905 | 0.2103 | .30954 | 0.4009 |
| 3493 | .58072 | 0.1653 | .17041 | 0.0827 | .23085 | 0.2303 | .31418 | 0.4383 |
| 3493 | .58072 | 0.1653 | .17041 | 0.0827 | .23085 | 0.2303 | .31418 | 0.4383 |
| 3571 | .58356 | 0.2797 | .17083 | 0.1398 | .23250 | 0.4176 | .31882 | 0.8957 |
| 3771 | .59679 | 0.5329 | .17276 | 0.2665 | .24052 | 0.8039 | .34317 | 1.7232 |
| 3971 | .61654 | 0.7187 | .17559 | 0.3594 | .25242 | 1.0470 | .39740 | 2.1073 |
| 4171 | .64087 | 0.8501 | .17902 | 0.4251 | .26674 | 1.1849 | .42237 | 2.2291 |
| 4371 | .66839 | 0.9394 | .18283 | 0.4697 | .28246 | 1.2514 | .46887 | 2.2158 |
| 4571 | .69804 | 0.9972 | .18684 | 0.4986 | .29891 | 1.2725 | .51695 | 2.1414 |
| 4771 | .72909 | 1.0321 | .19095 | 0.5161 | .31563 | 1.2664 | .56546 | 2.0457 |
| 4971 | .76097 | 1.0507 | .19508 | 0.5254 | .33235 | 1.2454 | .61380 | 1.9488 |
| 5171 | .79332 | 1.0584 | .19918 | 0.5293 | .34890 | 1.2177 | .66167 | 1.8607 |
| 5371 | .82586 | 1.0591 | .20323 | 0.5296 | .36519 | 1.1883 | .70905 | 1.7859 |
| 5387 | .82846 | 1.0590 | .20355 | 0.5296 | .36648 | 1.1860 | .71282 | 1.7805 |
| 5571 | .85843 | 1.0569 | .20720 | 0.5285 | .38122 | 1.1625 | .75605 | 1.7302 |
| 5721 | .88288 | 1.0586 | .21013 | 0.5294 | .39312 | 1.1530 | .79141 | 1.7155 |
| 5721 | .88288 | 1.0586 | .21013 | 0.5294 | .39312 | 1.1530 | .79141 | 1.7155 |
| 5771 | .89106 | 1.0618 | .21110 | 0.5309 | .39708 | 1.1548 | .80334 | 1.7226 |
| 5871 | .90753 | 1.0707 | .21304 | 0.5354 | .40507 | 1.1633 | .82763 | 1.7473 |
| 5958 | .92201 | 1.0811 | .21473 | 0.5406 | .41209 | 1.1753 | .84936 | 1.7782 |
| 5971 | .92418 | 1.0828 | .21499 | 0.5415 | .41315 | 1.1774 | .85266 | 1.7834 |
| 6021 | .93259 | 1.0902 | .21596 | 0.5452 | .41724 | 1.1867 | .86551 | 1.8059 |
| 6021 | .93259 | 1.0902 | .21596 | 0.5452 | .41724 | 1.1867 | .86551 | 1.8059 |
| 6071 | .94109 | 1.1037 | .21695 | 0.5519 | .42139 | 1.2064 | .87871 | 1.8530 |
| 6171 | .95841 | 1.1285 | .21893 | 0.5643 | .42991 | 1.2413 | .90633 | 1.9322 |
| 6271 | .97613 | 1.1501 | .22095 | 0.5751 | .43867 | 1.2695 | .93539 | 1.9916 |
| 6311 | .98332 | 1.1579 | .22176 | 0.5790 | .44224 | 1.2792 | .94737 | 2.0108 |
| 6356 | .99147 | 1.1666 | .22268 | 0.5834 | .44630 | 1.2895 | .96106 | 2.0301 |
| 6356 | .99147 | 1.1666 | .22268 | 0.5834 | .44630 | 1.2895 | .96106 | 2.0301 |
| 6371 | .99421 | 1.1726 | .22298 | 0.5864 | .44766 | 1.2980 | .96569 | 2.0486 |

both $f$ and $f'$, it is possible to generate a new difference equation to replace the one originally valid at the point of discontinuity in the first instance; similarly it is also possible to generate two new difference equations to replace the two original equations of the system in the immediate neighborhood of the discontinuity.

In the solution of the Clairaut equations, we have adopted the following procedure. Select an interval $H$ such that the discontinuity nearest the surface coincides with a pivotal point. This avoids involving the surface boundary condition with the calculations for the discontinuous coefficients. For both the $HB_1$ and the earlier Bullen model this constraint forces the other discontinuities not to coincide with any other pivotal point. Following the aforementioned remarks, we modified the original system (16) and solved it for the interval $H$ and $H/2^n$ by utilizing a subroutine of McCormick and Salvadori[7] valid for matrices in tridiagonal form. In order to offset the fact that we originally neglected third-order central differences in our approximation procedure, we have followed an iteration method aimed at refining the results. Thus, if $f_l$ represents a first approximation to our differential equation, then in order that $f_l + z_l$ represent a better approximation to the same differential equation, $z_l$ must satisfy a linear differential equation whose coefficients depend on $f_l$, provided that second and higher powers of $z_l$ are neglected. Solving this so-called "equation of variation" by the same procedure, we obtain $z_l$ to be added to $f_l$. The procedure can be repeated until the residual becomes insignificant and the solution converges.

Each of the six Clairaut equations to be solved was iterated at least twice to convergence before proceeding to solving the next one. The logarithmic derivative $\eta$ was calculated by numerical differentation of $f$. Observation of the results shows that the functions $f$ and $\eta$ for all six equations converge to at least four decimal places, with residual terms of the order of $10^{-10}$. As another test of convergence, the interval $H$ was halved and the process repeated for the same number of iterations until the changes in the final result was insignificant.

The results tabulated at the original data points are linear interpolations between the pivotal points: for $HB_1$ we have taken $N=851$ and performed five iterations, for the 1940 Bullen model we have $N=387$ and three iterations. Comparison of the tabulated values of the functions $f$ shows that the $HB_1$ results converge to at least the five digits shown in Table 2. The values of the $K(a_l)$, $f(a_l)$, and of the ellipticity are straightforward calculations from the solutions at the surface. The moments of inertia $C=I_p$, $A=I_e$ and the ratio $(C-A)/C$ are obtained from integration via trapezoidal rule of the functions using the pivotal point values.

The just-described computations were programmed in Fortran and executed at the Naval Research Laboratory on the Texas Instruments ASC-7 computer in double precision floating point arithmetic to a precision of 16 decimal digits. Observation of the finite differences involved indicates a minimum of 10 digits are needed to retain significance in the range nearest to the Earth's core where $D \sim 1$. This region is also where the largest discrepancy occurs between our calculations and the 1963 results of James and Kopal for the 1940 Bullen model.

## IV. Geodetic Results

We have integrated numerically the Clairaut equations for both the 1940 Bullen Earth model and the 1969 $HB_1$ model using 387 and 851 pivotal points, respectively. Table 2 provides the values for the deformation coefficients $f_0(a)$, $f_2(a)$, $f_4(a)$, $f_6(a)$ and their logarithmic derivatives $\eta(a)$ at the data points of the $HB_1$ model from the center of the Earth, $a=0$, to its surface $a=6371$ km. Thus, the shape of the equipotential surfaces throughout the interior of the Earth has been ascertained.

Once the $f$'s are known to their third-order approximation, one can evaluate the moments of inertia (polar $C=I_p$, and equatorial $A=I_e$), as well as the coefficients $K_2$, $K_4$, $K_6$ which appear in the exterior potential

$$V(r,\nu;a_l) = \frac{Gm_l}{r}\left[1+\sum_{j=1}^{3} K_{2j}(a_l)\left(\frac{a_l}{r}\right)^{2j} P_{2j}(\nu)\right] \quad (18)$$

to the same order of approximation by using the relations given in Lanzano.[1] The ellipticity can be calculated from Eq. (1) as

$$\epsilon = \frac{r(a_l,0) - r(a_l,1)}{r(a_l,0)}$$

Table 3 gives the surface values of the $HB_1$ and the 1940 Bullen model and compares them to Kopal's 1963 results where the Bullen model was used but only the second-order Clairaut approximation was available.

By replacing the values $f_0(a_l)$, $f_2(a_l)$, $f_4(a_l)$, and $f_6(a_l)$ for the $HB_1$ model into Eq. (1), we get the equation of the geoid according to the most advanced density model yet available. Satellite altimetry requires that we know the geoid to less than one meter. In our opinion, this could be achieved if we adopted this newly developed sixth-order geoid as the reference spheroid instead of the old international ellipsoid in all gravimetric work in conjunction with Stokes' formula (see, e.g., Heiskanen and Moritz[8]).

Let us compare the coefficients of the harmonics in the exterior potential with the 1969 Kozai[9] values adopted in satellite geodesy. The $K_2$ values for both density models encompass the satellite value $0.10826 \cdot 10^{-2}$, our $K_4$ values are almost twice as large as the satellite value $0.15930 \cdot 10^{-5}$, whereas the $K_6$ values are one order of magnitude smaller than the satellite value $5.0200 \cdot 10^{-7}$. The two values for $\epsilon^{-1}$ also encompass the 298.2 value accepted from satellite theory. The same can be said about the ratio $(C-A)/C$ for the two models with respect to the value $0.3272 \cdot 10^{-2}$ obtainable from the precessional constant. The two moments of interia for the $HB_1$ model yield the following ratios: $C/m_l a_l^2 = 0.331762$ and $A/m_l a_l^2 = 0.330686$ as compared with the accepted values

**Table 3 Comparison of Earth density models**

| Parameter | $HB_1$ ($N=851$) | Bullen (1940) ($N=387$) | James and Kopal (1963) |
|---|---|---|---|
| $f_0(a_l)$ | $-0.99421 \cdot 10^{-6}$ | $-0.10098 \cdot 10^{-5}$ | $-0.10 \cdot 10^{-5}$ |
| $f_2(a_l)$ | $-0.22298 \cdot 10^{-2}$ | $-0.22473 \cdot 10^{-2}$ | $-0.22504 \cdot 10^{-2}$ |
| $f_4(a_l)$ | $+0.44766 \cdot 10^{-5}$ | $+0.45202 \cdot 10^{-5}$ | $+0.45 \cdot 10^{-5}$ |
| $f_6(a_l)$ | $-0.96569 \cdot 10^{-8}$ | $-0.97129 \cdot 10^{-8}$ | ... |
| $K_2(a_l)$ | $-0.10756 \cdot 10^{-2}$ | $-0.10929 \cdot 10^{-2}$ | $-0.10961 \cdot 10^{-2}$ |
| $K_4(a_l)$ | $+0.29776 \cdot 10^{-5}$ | $+0.30495 \cdot 10^{-5}$ | $+0.315 \cdot 10^{-5}$ |
| $K_6(a_l)$ | $-0.11293 \cdot 10^{-7}$ | $-0.11598 \cdot 10^{-7}$ | ... |
| $\epsilon^{-1}$ | 299.6 | 297.2 | 296.8 |
| $A=I_e$ | $0.80212428 \cdot 10^{35}$ | $0.80893171 \cdot 10^{35}$ | $0.81078966 \cdot 10^{35}$ |
| $C=I_p$ | $0.80473398 \cdot 10^{35}$ | $0.81158858 \cdot 10^{35}$ | $0.81346066 \cdot 10^{35}$ |
| $(C-A)/C$ | $0.3243 \cdot 10^{-2}$ | $0.3274 \cdot 10^{-2}$ | $0.3282 \cdot 10^{-2}$ |

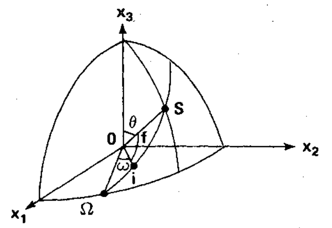


**Fig. 1 Elements of a Keplerian elliptic orbit.**

0.33089 and 0.32981, respectively, obtainable from satellite theory. These discrepancies can be attributed to the deviation of the Earth's interior from hydrostatic equilibrium and the existence of shearing stresses due to convection currents in the Earth's mantle.

A few remarks are appropriate. 1) Note the variation in the surface values between the 1940 Bullen and the 1969 $HB_1$ Earth model; it is expected that new seismological data will in the near future contribute to a more accurate model. 2) Comparison of data obtainable from two different sources (i.e., satellite and density) can be used to test the validity of certain assumptions concerning the layers of the Earth's interior. 3) Use of more precise formulas and more accurate statistical methods in handling large numbers of satellite data might bring some changes to the results of satellite geodesy.

## V. Secular Variations of Orbital Elements

Various procedures have been advocated in the past for extracting information of geophysical interest by examining satellite data (see, e.g., Kaula[10]). In our opinion, the most accurate way for obtaining the $K_2, K_4, K_6$ values from satellite data is to use the secular variations of the orbital elements. For this purpose, we proceed in this section to obtain analytically such expressions by using the Lagrangian perturbation equations of celestial mechanics.[11]

Consider an orthogonal reference system $(0;X_1,X_2,X_3)$ with origin 0 at the centroid of the body, the $X_1,X_2$ axes lying in the equatorial plane, the $X_1$ axis pointing toward the first point of Aries, and the $X_3$ axis being rotational axis. Figure 1 represents the unperturbed Keplerian elliptic orbit in a general position with respect to said reference. The elements pertaining to this elliptic orbit are denoted as follows:

| | |
|---|---|
| $\Omega$ | = longitude of the node |
| $i$ | = inclination of orbital plane to equatorial plane |
| $\omega$ | = argument of periastron |
| $f$ | = true anomaly |
| $A$ | = semimajor axis |
| $e<1$ | = eccentricity |
| $L$ | $= A(1-e^2)$ = semilatus rectum |
| $\mu$ | $= Gm_1$ = gravitational parameter |
| $M$ | $= nt+\chi$ = mean anomaly, where $t$ is the time and $n$ the mean angular motion |

The Lagrangian perturbation equations express the time derivatives of the orbital elements in terms of the 1) orbital elements themselves, and 2) partial derivatives of the exterior potential with respect to these elements.

To obtain the secular variations experienced by the orbital elements, one must: 1) express the potential $V$ in terms of the time through the mean anomaly $M$, 2) take the derivatives of this expansion with respect to the prescribed elements, and 3) isolate the nonperiodic terms. This must be done for each of the harmonics in consideration.

Any even-order harmonic can be written as

$$V_{2j}(r,\nu;\alpha_1) = A_j\left(\frac{A}{r}\right)^{2j+1} P_{2j}(\nu) \qquad (19)$$

where

$$A_j = \frac{\mu}{\alpha_1} K_{2j}(\alpha_1)\left(\frac{\alpha_1}{A}\right)^{2j+1} \qquad (20)$$

and the $P$'s are the Legendre polynomials. From Fig. 1, we have

$$\nu = \cos\theta = \sin(i)\,\sin(\omega+f) \qquad (21)$$

which allows the transition from $\theta$ to $f$. Using the addition theorem of the Legendre polynomials, see e.g., MacRobert,[12] we can write

$$P_{2j}(\nu) = \sum_{k=0}^{j} B_{jk} P_{2j}^{2k}(\cos i)\,\cos(2kf+2k\omega-k\pi) \qquad (22)$$

where

$$B_{jk} = u_{2k}\frac{(2j-2k)!}{(2j+2k)!} P_{2j}^{2k}(0) \qquad (23)$$

with $u_0 = 1$, $u_{2k} = 2$ for $k \neq 0$ and the

$$P_n^m(x) = (1-x^2)^{m/2} P_n^{(m)}(x) \qquad (24)$$

are the Legendre functions of the first kind defined in terms of the derivatives of the Legendre polynomials.

In Eq. (22) account has been taken of the fact that $P_n^m(0) = 0$ when $n-m$ is an odd number. The next transition from true anomaly $f$ to mean anomaly $M$ and thence to time is performed by means of certain infinite expansions (see Plummer[13] and Groves[14]) which can be written as follows:

$$(1+\beta^2)^{-2j}\left(\frac{A}{r}\right)^{2j+1}\cos(2kf+\delta)$$

$$= \sum_{\ell=-\infty}^{\infty}\ \sum_{h=-\infty}^{\infty} X_{\ell,h}^{-(2j+1),2k}(\beta) J_h(\ell e)\cos(\ell M+\delta) \qquad (25)$$

Here $\beta = \tan(\alpha/2)$, with $\sin\alpha = e$, is a variable depending on the eccentricity, and the $J$'s are Bessel functions. The $X$'s are the Hansen coefficients and can be represented as hypergeometric polynomials. The validity of Eq. (25) depends on the exponent of $A/r$ and the coefficient of $f$ being integers.

To obtain a secular, i.e., nonperiodic, term one must take $\ell = 0$ in Eq. (25). Since $J_h(0)$ is one, if $h=0$, and zero, if $h \neq 0$, we can limit ourselves to choosing $h=0$. Thus, the only contribution of the series (25) toward a secular term is obtained by taking $\ell = h = 0$.

Let us remark at this point that: 1) $\partial V/\partial\chi$ consists of terms like $\ell\,\sin(\ell M+\delta)$ and will not produce any secular contribution, and 2) we can replace $\ell = h = 0$ in the foregoing series before performing the prerequisite partial derivatives.

Using results due to Lanzano,[15] it is possible to express the relevant Hansen coefficients as Legendre functions of the first kind according to

$$(1+\beta^2)^{2j} X_{0,0}^{-(2j+1),2k}(\beta) = \frac{(-1)^k(2j-1)!}{(2j+2k-1)!}\gamma^{2j} P_{2j-1}^{2k}(\gamma) \qquad (26)$$

where

$$\gamma = \frac{1+\beta^2}{1-\beta^2} = (1-e^2)^{-1/2} \qquad (27)$$

Thus, to obtain the secular terms, we must take the partial derivatives of the following expression

$$A_j \sum_{k=0}^{j-1} C_{jk} P_{2j}^{2k}(\cos i)\gamma^{2j} P_{2j-1}^{2k}(\gamma)\cos(k\pi - 2k\omega) \qquad (28)$$

where

$$C_{jk} = \frac{(-1)^k(2j-1)!}{(2j-1+2k)!} B_{jk} \qquad (29)$$

**Table 4 Secular variations of orbital elements $e$, $\Omega$, and $\omega$ ($C=\cos^2 i$)**

$$[\dot{e}_n]=\left(\frac{\mu}{A^3}\right)^{1/2}\left(\frac{a_I}{L}\right)^n K_n(a_I)e(1-e^2)(1-C)E_n$$

| $n$ | $E_n$ |
|---|---|
| 4 | $\frac{15}{32}(7C-1)\sin 2\omega$ |
| 6 | $\frac{-105}{1024}[5(2+e^2)(33C^2-18C+1)\sin 2\omega + 3e^2(1-C)(11C-1)\sin 4\omega]$ |

$$[\dot{\Omega}_n]=\left(\frac{\mu}{A^3}\right)^{1/2}\left(\frac{a_I}{L}\right)^n K_n(a_I)\cos i\ F_n$$

| $n$ | $F_n$ |
|---|---|
| 2 | 3/2 |
| 4 | $\frac{-15}{16}\left[(1+\frac{3}{2}e^2)(7C-3)-e^2(7C-4)\cos 2\omega\right]$ |
| 6 | $\frac{105}{1024}\left[\left(8+40e^2+15e^4\right)\left(33C^2-30C+5\right) - 5e^2(2+e^2)(99C^2-102C+19)\cos 2\omega - \frac{3}{2}e^4(1-C)(33C-13)\cos 4\omega\right]$ |

$$[\dot{\omega}_n]+[\dot{\Omega}_n]\cos i=\left(\frac{\mu}{A^3}\right)^{1/2}\left(\frac{a_I}{L}\right)^n K_n(a_I)G_n$$

| $n$ | $G_n$ |
|---|---|
| 2 | $\frac{3}{4}(1-3C)$ |
| 4 | $\frac{15}{128}\left[(4+3e^2)(35C^2-30C+3) + 2(2+5e^2)(1-C)(7C-1)\cos 2\omega\right]$ |
| 6 | $\frac{-105}{2048}\left[(8+20e^2+5e^4)(231C^3-315C^2+105C-5) + 5(4+22e^2+7e^4)(1-C)(33C^2-18C+1)\cos 2\omega + \frac{3}{2}e^2(4+7e^2)(1-C)^2(11C-1)\cos 4\omega\right]$ |

with respect to the orbital elements. This expression depends on $\omega$, $i$, and $e$ through the $\gamma$, but does not depend on $\Omega$.

In what follows, a bracket around the time derivative of an element shall denote its secular variation. By examining the Lagrangian equations and making use of the preceding remarks, we can say at once that

$$[\dot{A}_{2j}]=0 \tag{30a}$$

$$[\dot{e}_2]=0 \tag{30b}$$

$$[\mathrm{d}i_{2j}/\mathrm{d}t]=-\{e/(1-e^2)\}(\cot i)[\dot{e}_{2j}] \tag{30c}$$

The nonvanishing terms are presented in Table 4, where for typographical simplicity we have set $C=\cos^2 i$. Because of their explicit dependence on the orbital elements, these expressions can be utilized to attain a better determination of the geopotential from the observed secular variations of satellite motion.

## VI. Application to Planetology

To conclude, we mention the fact that the Clairaut equation is applicable to the study of the equilibrium configuration of the giant planets Jupiter and Saturn because hydrostatic equilibrium is a more acceptable hypothesis for their interiors. Furthermore, the rotational parameter $q$ is 0.028 for Jupiter and 0.047 for Saturn, that is to say, one order of magnitude higher than the Earth's. We might expect, therefore, that the third-order theory when applied to these planets should yield more accurate results than the second-order theory used by James and Kopal[3] in conjunction with the DeMarcus density data.

The main question still in debate for these planets is their internal density distribution. The most plausible approach, in our opinion, is to consider the planet as a polytrope of given index $n$, so that the pressure $p$ and density $\rho$ are related according to

$$p=K\rho^{1+1/n} \tag{31}$$

$K$ being a constant. This condition, when coupled with hydrostatic equilibrium leads to a potential

$$V=V_0+K(n+1)\rho^{1/n} \tag{32}$$

where $V_0$ is a constant of integration. The use of the Poisson equation finally leads to the fundamental equation

$$(1/a^2)(a^2\theta')'=-h\theta^n+k \tag{33}$$

where $\theta^n=\rho/\rho_c$ and primes denote, as usual, derivatives with respect to the radius $a$. The parameters $h$ and $k$ are two constants, $k$ depending on the rotational velocity $\omega_I$. Because of the appearance of the last term on the right-hand side, Eq. (33) is a nonhomogeneous Lane-Emden equation: its homogeneous counterpart has been studied extensively in the astrophysical literature (see e.g., Cox and Giuli[16]).

Because of the differential rotation exhibited by Jupiter, a parametric study of Eq. (33) should be undertaken for various recorded values of $\omega_I$ according to latitude. Numerical integration of Eq. (33) for a given value of $n$, with $0<n<5$, will provide $\rho(a)$. The selection of a value for the polytropic index $n$ should be dictated by a compromise on the value of the radius, total mass, central density, and pressure within the planet. Once $\rho(a)$ is ascertained with a certain degree of confidence, the Clairaut equation can be used to study the gravity field of the planet.

## Acknowledgments

This research was sponsored by The Office of Naval Research. The authors express their appreciation to Mrs. B. McDonald for preparing the final manuscript, and to N. W. Guinard, Superintendent, Space Systems Division, for making possible the collaboration between the authors.

## References

[1] Lanzano, P., "The Equilibrium of a Rotating Body of Arbitrary Density," *Astrophysics and Space Science*, Vol. 29, July 1974, pp. 161-178.

[2] Bullen, K. E., *Introduction to the Theory of Seismology*, 3rd rev. ed., Cambridge University Press, 1965, pp. 227-240.

[3] James, R. and Kopal, Z., "The Equilibrium Figures of the Earth and the Major Planets," *Icarus*, Vol. 1, April 1963, pp. 442-454.

[4] Haddon, R. A. W. and Bullen, K. E., "An Earth Model Incorporating Free Earth Oscillation Data," *Physics of the Earth and Planetary Interiors*, Vol. 2, Jan. 1969, pp. 35-49.

[5] McCalla, T. R., *Introduction to Numerical Methods and Fortran Programming*, John Wiley, New York, 1967, pp. 294-297.

[6]Fox, L., *The Numerical Solution of Two-Point Boundary Problems*, Oxford University Press, 1957, pp. 67-68, and 328-332.
[7]McCormick, J. M. and Salvadori, M. G., *Numerical Methods in Fortran*, Prentice-Hall, Englewood Cliffs, N.J., 1964, pp. 223-226.
[8]Heiskanen, W. A. and Moritz, H., *Physical Geodesy*, Freeman, San Francisco, 1967, pp. 94-98.
[9]Kozai, Y., "Revised Values for Coefficients of Zonal Harmonics in the Geopotential," Spec. Rept. 295, Smithsonian Astrophysics Observatory, Cambridge, Mass., 1969, p. 17.
[10]Kaula, W. M., *Theory of Satellite Geodesy*, Blaisdell, Waltham, Mass., 1966, pp. 116-120.
[11]Smart, W. M., *Celestial Mechanics*, Longmans, Green, London, 1953, p. 69.
[12]MacRobert, T. M., *Sperical Harmonics*, 2nd rev. ed., Dover, New York, 1948, p. 138.
[13]Plummer, H. C., *An Introductory Treatise on Dynamical Astronomy*, Dover, New York, 1960, pp. 44-46.
[14]Groves, G. V., "Motion of a Satellite in the Earth's Gravitational Field," *Proceedings of the Royal Society, London*, Vol. 254, Jan. 1960, pp. 48-65.
[15]Lanzano, P., "A Third-Order Theory for the Equilibrium Configuration of a Rotating Planet," *Icarus*, Vol. 1, Sept. 1962, pp. 121-136.
[16]Cox, J. P. and Giuli, R. T., *Principles of Stellar Structure*, Gordon and Breach, New York, 1968, pp. 704-713.